

GoDe: Gaussians on Demand for Progressive Level of Detail and Scalable Compression

Francesco Di Sario
University of Turin, Italy
francesco.disario@unito.it

Riccardo Renzulli
University of Turin, Italy
riccardo.renzulli@unito.it

Marco Grangetto
University of Turin, Italy
marco.grangetto@unito.it

Akihiro Sugimoto
National Institute of Informatics, Japan
sugimoto@nii.ac.jp

Enzo Tartaglione
LTCI, Télécom Paris, Institut Polytechnique de Paris, France
enzo.tartaglione@telecom-paris.fr

Abstract

3D Gaussian Splatting enhances real-time performance in novel view synthesis by representing scenes with mixtures of Gaussians and utilizing differentiable rasterization. However, it typically requires large storage capacity and high VRAM, demanding the design of effective pruning and compression techniques. Existing methods, while effective in some scenarios, struggle with scalability and fail to adapt models based on critical factors such as computing capabilities or bandwidth, requiring to re-train the model under different configurations. In this work, we propose a novel, model-agnostic technique that organizes Gaussians into several hierarchical layers, enabling progressive Level of Detail (LoD) strategy. This method, combined with recent approach of compression of 3DGS, allows a single model to instantly scale across several compression ratios, with minimal to none impact to quality compared to a single non-scalable model and without requiring re-training. We validate our approach on typical datasets and benchmarks, showcasing low distortion and substantial gains in terms of scalability and adaptability. The source code, provided in the supplementary material, will be open-sourced upon acceptance of the paper.

1. Introduction

Neural Radiance Fields (NeRFs) [25] have consistently boosted novel view synthesis, achieving state-of-the-art quality in scene reconstruction. However, its limitations lie in slow training and inference times. Over the last

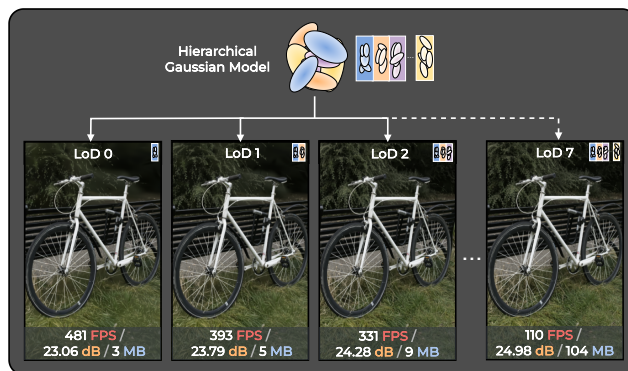


Figure 1. Our method constructs a progressive hierarchy of Gaussians, enabling progressive LoD. Combined with compression techniques, this allows the model to operate across several (eight in the figure) compression rates, ranging from extremely high to low. The model can dynamically adjust the rate based on criteria such as a target minimum FPS.

few years, different methods [5, 12, 13, 16, 27, 33] have been proposed to enhance speed, but none have successfully achieved real-time performance for complex, high-resolution scenes. 3D Gaussian Splatting (3DGS) [17] represents a major advancement by modeling scenes as mixtures of Gaussians, effectively replacing the computationally intensive tasks of ray casting, ray sampling, and neural network queries. By leveraging differentiable rasterization and spherical harmonics for handling view-dependent effects, 3DGS achieves real-time performance even in complex real-world scenarios and at high-definition resolution. 3DGS offers competitive training times and reconstruct-

tion quality that can rival or even surpass that of NeRF-based models. Despite these advancements, some challenges still persist. Specifically, 3DGS models often require large storage and VRAM resources, as scene representations may involve millions of Gaussians. This may hinder real-time rendering on consumer-level devices and make on-demand streaming of 3DGS model quite prohibitive. This has sparked interest in pruning and compression techniques to reduce VRAM consumption during runtime and minimize storage requirements, with high rendering quality. While current pruning and compression methods [1, 2, 11, 14, 29, 37] have shown effectiveness in improving performance and reducing VRAM usage, they lack *scalability*: they require further optimization and personalization for each specific compression level, resulting in multiple models, one for each compression level.

To address this scalability issue, we propose GoDe (**G**aussians **o**n **D**emand), a novel approach that enables scalable compression. As shown in Fig. 1, GoDe enables a 3DGS model to scale across different compression rates, without the need for retraining specialized models. Specifically, GoDe employs a progressive Level of Detail (LoD) approach: Gaussians are organized into discrete and progressive levels, with each level adding more detail (enhancement) to the previous one. This progressive structure allows 3DGS models to be highly scalable across different scenarios. In fact, by adding or removing enhancement layers, we can easily adjust the trade-off between quality and performance. When combined with compression technique schemes, this approach enables scalable compression. Each level of detail can be seen as a distinct compression level, where higher LoDs corresponds to lower compression rate and lower LoDs corresponds to a higher compression rate. This allows for navigating the rate/distortion curve by simply adding or removing enhancement layers. To build the hierarchy, inspired by iterative gradient-informed pruning approaches, we developed an iterative gradient-informed masking methods that progressively constructs the hierarchy in a top-down manner (from high to low levels). This methods is general and compatible with popular 3DGS baselines. A fine-tuning phase ensures coherence and smoothness across the levels, while a final compression stage further reduce model size.

In summary, our main contributions are:

- **A general method for progressive LoD** (Sec. 3.1): Leveraging a novel gradient-based iterative masking technique, we show the applicability of this method to a variety of popular 3DGS model (Sec. 4.2) and how this approach effectively organizes primitives into a hierarchy of progressive levels with respect to other approaches (Sec. 4.4.2).
- **Smooth transition between levels** (Sec. 3.2): Our fine-tuning procedure offers a simple and effective way to

reduce artifacts between levels, ensuring smooth transitions in visual fidelity across multiple LoDs (Sec. 4.3) and boosting LoD quality (Sect. 4.4.3).

- **Scalable Compression** (Sec. 3.3): Our method integrates and extends state-of-the-art compression techniques, enabling scalable compression and adaptive rendering, with comparable and sometimes even superior performance of non-scalable methods (Sec. 4.4.4).

We extensively evaluate our approach on standard benchmark and compared it against the most recent state-of-the-art methods, showing comparable and even superior performances than non-scalable method. Our method allows models to scale across a wide range of compression levels, from low to very high, achieving up to 99.76% reduction in model size and 98.36% in the number of primitives in the highest compression rate with respect to non-compressed models, while preserving comparable full-size model quality at the lowest compression rate.

2. Background and Related Work

2.1. 3DGS Preliminaries

3DGS [17] has emerged as a cutting-edge technique for real-time radiance field rendering, delivering top-tier performance in both quality and speed. It represents a scene using volumetric Gaussian primitives, each defined by a set of parameters: a position \mathbf{x} , a covariance matrix Σ , which is decomposed into scaling and rotation components, an opacity o , and Spherical Harmonics (SH) coefficients to capture view-dependent color or appearance. In the rendering stage, the 3D primitives are projected into 2D screen space and rasterized with alpha blending $\alpha = oG$ [39] with the projected Gaussian’s contribution to position \mathbf{x} given by $G(\mathbf{x}) = \exp(-\frac{1}{2}(\mathbf{x}^T)\Sigma^{-1}(\mathbf{x}^T))$. The combined effect of converting SHs to per-view color values and applying alpha blending reconstructs the appearance of the captured scene. These primitives originate from a sparse Structure-from-Motion (SfM) point cloud and are optimized through a gradient-descent process, combined with adaptive refinements. This ensures the optimization of both pixel-wise similarity and structural similarity.

2.2. 3DGS Level of Detail

LoD is a well-established technique in computer graphics, used to optimize performance and improve visual quality. It comprises three main components: constructing a scene representation at various levels of detail, implementing a policy for selecting the appropriate level based on the view, and enabling seamless transitions between levels to avoid artifacts or noticeable stuttering. Recent works have integrated LoD techniques with 3DGS, mainly to reduce aliasing artifacts [38] and improve performance, especially for large-scale datasets [23]. These methods typically involve

learning multiple levels of detail within the scene representation, followed by selective rendering according to heuristics like pixel coverage (i.e., the number of pixels occupied by a Gaussian projection on the image plane) and distance. Other work propose a hierarchical representation, often structured as a tree, as proposed by [18, 24]. This method dynamically implements LoD by selectively rendering Gaussians up to a specific level within the structure based on certain heuristics. In these approaches, LoD is typically defined at render time (dynamic LoD), which complicates its integration into compression contexts like ours, where a predefined, discrete set of progressive enhancement layers is essential. Additionally, these dynamic LoD methods often introduce significant overhead due to the need for tree traversal algorithms to construct levels of detail, as opposed to the simpler and faster operation of layer concatenation, which is more suitable for adaptive rendering in bandwidth-limited scenarios.

2.3. 3DGS Compression

Since the introduction of hybrid radiance fields models that incorporate auxiliary data structures to accelerate training and inference times, such as voxel grids [5, 13, 28, 33], research has focused on compression [8] and complexity reduction [9]. For instance, [8] demonstrates how an iterative-magnitude pruning approach is highly effective in reducing the number of parameters even in the context of radiance fields. These techniques have recently been adapted in the field of 3DGS. In fact, despite its advantages, 3DGS is limited by high storage and memory demands, reducing its application, for example, on low-end hardware. Current compression methods aim at achieving the highest quality at minimal storage size. Typically, compact representations involve post-hoc Gaussian pruning followed by compression stages, including quantization and entropy coding [1, 10, 30, 36]. Some methods operate directly during training, aiming to limit the number of Gaussians via learned masks and optimized encoding schemes [6, 14, 22, 31, 34]. Other studies enhance the representation by employing neural networks for on-the-fly Gaussian generation [24], tri-planes [35], or by using auxiliary structures such as hash grids to store spherical harmonics [6, 21], further reducing storage demands. In particular, Scaffold-GS [24] reduces storage by up to 5 times by replacing Gaussians with anchor points. These anchor points, which are significantly fewer in number, are associated with a set of features, offsets, and scalings. A set of shallow neural networks process each anchor point and generates the parameters of view-adaptive Gaussians. However, it is important to note that none of these methods are scalable in practice. While different compression rates can be achieved, they require retraining the model from scratch or performing additional fine-tuning steps for each com-

pression level. This limitation makes it difficult to adapt these model across a broad range of context, such as low bandwidth or varying hardware capabilities. In contrast, our method incorporates a scalable compression scheme: with a single training we can instantly obtain different compression levels, effectively navigating the rate-distortion curve. Furthermore, our method matches or even surpass dedicated, non-scalable compression techniques.

3. Gaussians on demand

This section presents our proposed efficient and adaptive 3D rendering method using hierarchical Gaussian representations. The proposed approach extends the standard 3D Gaussian Splatting (3DGS) framework by introducing a hierarchical representation of the scene at multiple levels of detail. The objective is to develop a single, scalable model that can dynamically adapt to various criteria, such as computational resources or available bandwidth. We present a novel algorithm that implicitly constructs this hierarchy, enabling a single 3DGS model to learn multiple levels of detail. We first describe how to build a progressive hierarchy of Gaussians from a pre-trained 3DGS model (Sec. 3.1). Then, we show how to train and fine-tune Gaussians in different levels of detail (Sec. 3.2). Finally, we describe our scalable compression and adaptive rendering steps (Sec. 3.3).

3.1. Hierarchy of Gaussians

Let L denote the total number of levels of detail in the hierarchy. To implement progressive LoD, our objective is to organize the Gaussians of model \mathcal{G} as a sequence of progressive levels $l \in \{0, \dots, L - 1\}$ defined as

$$\mathcal{G} = (\mathcal{G}_0, \mathcal{E}_1, \dots, \mathcal{E}_l, \dots, \mathcal{E}_{L-1}), \quad (1)$$

where \mathcal{G}_0 denotes a set of starting Gaussians, and \mathcal{E}_l is the set of enhancement Gaussians at level l . We also refer to \mathcal{G} as \mathcal{G}_{L-1} . The progressive LoD \mathcal{G}_l at a given level l is defined as:

$$\mathcal{G}_l = \mathcal{G}_0 \cup \bigcup_{i=1}^l \mathcal{E}_i. \quad (2)$$

The sets are organized progressively, ensuring that

$$\mathcal{G}_0 \cap \mathcal{E}_1, \dots, \cap \mathcal{E}_l, \dots, \cap \mathcal{E}_{L-1} = \emptyset. \quad (3)$$

This guarantees that each level of detail progressively introduces new Gaussians, with no overlap among the layers. In order to define how many Gaussians are associated with each enhancement set, we define the number of Gaussians $|\mathcal{G}_l|$ associated with level of detail l as:

$$|\mathcal{G}_l| = c_{\min} \cdot b^l, \quad (4)$$

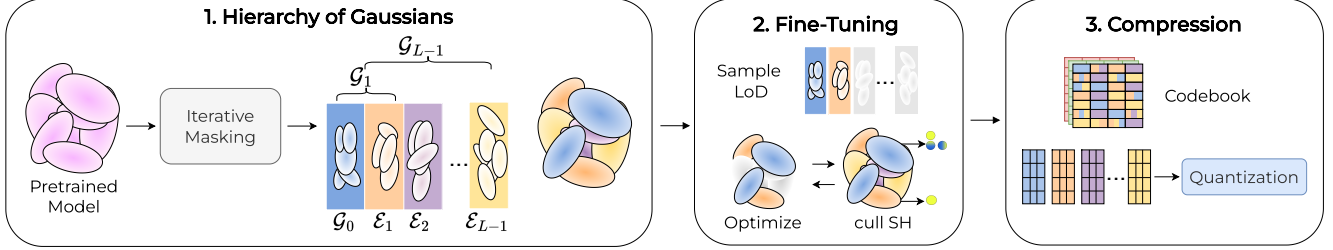


Figure 2. Graphical overview of our method GoDe. 1) Starting from a pre-trained model, we build a progressive hierarchy of Gaussians through iterative gradient-informed masking. 2) A fine-tuning stage further enhances the model’s quality and reduces its memory footprint by culling unnecessary SH coefficients. 3) The model is further compressed through codebook quantization.

where b is computed as

$$b = \exp\left(\frac{\log(|\mathcal{G}_{L-1}|) - \log(c_{\min})}{L-1}\right) \quad (5)$$

and $c_{\min} = |\mathcal{G}_0|$ is the number of Gaussians at the first LoD level (chosen as desired). We choose this progression since the rate-distortion functions generally follow a logarithmic law (see the theoretical rate-distortion curve for a Gaussian source [7]).

To organize the Gaussians of the model into a hierarchical structure, we employ an iterative gradient-informed masking process. This approach follows a top-down strategy, starting with the construction of the higher enhancement levels first, namely, progressively building the model’s hierarchy from layer $l = L - 1$ to layer $l = 1$. The gradient of each parameter in the Gaussians serves as a critical and general indicator of its relevance to the overall model. A Gaussian with a low gradient indicates minimal contribution to the loss function. Conversely, a high gradient suggests that the Gaussian is essential and has a significant impact on the loss. We can then leverage gradient information to build a hierarchy. Specifically, to create the enhancement set \mathcal{E}_l , we accumulate gradients on \mathcal{G}_l using the training set in order to select the k_l Gaussians with the lowest importance score defined as the sum of the norm of the gradient of all parameters of each Gaussian:

$$\mathcal{E}_l = \text{lowest}_{k_l} \left\{ \left\| \frac{\partial \mathcal{L}}{\partial \theta_i} \right\|_2 \right\}_{i \in \mathcal{G}_l}, \quad (6)$$

where, with some abuse of notation, lowest_{k_l} denotes the set of the k_l Gaussians with the lowest importance. Note that the difference $|\mathcal{G}_l| - |\mathcal{G}_{l-1}|$ is our k_l . The selected Gaussians will be associated with \mathcal{E}_l and excluded (masked) from the next iterations. We reset the gradients and repeat the process. At the end of this iterative process, important Gaussians (with high gradient values) are placed at lower layers, while less important Gaussians are assigned to higher levels, where they model finer details and geometries. Although this phase requires $L - 1$ steps, it tends to

be very fast (1-2 minutes in total to build the hierarchy) as it only requires a single pass through the training set per step.

3.2. Fine-Tuning and SHs culling

This phase involves F fine-tuning iterations designed to improve reconstruction quality and enforce a smooth transition between levels of detail. A random level l is uniformly sampled at each iteration and a fine-tuning iteration is performed only on the \mathcal{G}_l Gaussians associated with the selected level l . This optimization further improves reconstruction quality, especially at the lower levels. During fine-tuning, Gaussian parameters are reduced by selectively culling the spherical harmonics. Following the approach proposed by [31], SH coefficients are analyzed halfway through the fine-tuning phase to identify which primitives can be represented with 0, 1, 2, or 3 bands. The SH function is evaluated across all input views to determine whether a primitive requires view-dependent effects, based on the extent of color variation between views. If a primitive maintains a consistent color across all views, view-dependent effects are considered unnecessary. In addition, higher-order bands can be discarded if the color remains stable with lower-order SH coefficients. This phase significantly reduces the model’s memory cost (with negligible quality loss) since each Gaussian is represented by 59 32-bit floating point numbers, of which 45 are dedicated to the SH coefficients.

3.3. Scalable Compression

After fine-tuning, the compression step is performed. Compression is applied independently to the first LoD \mathcal{G}_0 and the following enhancements \mathcal{E}_l . Initially, a codebook is generated for each parameter (excluding the position of the primitives) using K -means clustering. In particular, following [31], codebooks of 256 entries are created for the opacity, the three scaling components, the real and imaginary parts of the rotation quaternion, the base color coefficients, and one for the 3-channel color component for each of the 15 SH coefficient groups. Codebook entries and positions are further quantized to 16-bit half-precision floats: in this way, we

have achieved scalability since every LoD can be progressively decoded starting from the base one. It is worth pointing out that we move along the rate/distortion curve by just concatenating further enhancements. As shown in Sec. 4, our results are very competitive with the recent state-of-the-art, with the added value of a single scalable model obtained with a single training process. In conclusion, GoDe achieves both scalable compression and progressive LoD. Scalable compression can be exploited in many application scenarios beyond the simple memory-saving result, *e.g.* adaptive HTTP streaming [32]. The hierarchical organization of GoDe enhancements can be exploited for adaptive rendering at different LoD: specifically, the enhancements can be progressively splatted until a given target criterion, *e.g.* minimum frame rendering rate, is met. If rendering speed is the only goal, the GoDe compression phase can be skipped.

4. Experiments

4.1. Setup

The code was developed in Python 3.9 using PyTorch 2.1 and executed on a single NVIDIA A40 GPU. We set $L = 8$ for all the configurations, $c_{\min} = 100,000$. The fine-tuning phase comprises $F = 30,000$ iterations. All the other parameters remain unchanged from the original implementation. Our method was tested with three popular 3D Gaussian Splatting models: 3DGS [17], MCMC-3DGS [19], a variant of 3DGS that treats 3D Gaussians as samples from a Markov Chain Monte Carlo process, generally yielding slightly better results than 3DGS, and the neural-based Scaffold-GS [24]. For Scaffold-GS, due to its unique architecture, we adopted a slightly different compression scheme. This approach is similar to our proposed GoDe method but excludes SHs culling since SHs are not present in the model. Instead, it incorporates iterative masking with quantization-aware fine-tuning and entropy coding. The iterative masking process follows a similar approach; however, rather than masking Gaussians, we mask anchor points directly, evaluating the gradients of their respective features. Quantization is performed during the fine-tuning phase: features are quantized to 8-bit unsigned integers, while the scaling, offset, and positional attributes are quantized to half-precision floating points similarly to [30]. After fine-tuning, the model parameters are further compressed using ZIP, which combines LZ77 compression with Huffman entropy coding to achieve efficient and lossless storage reduction.

4.2. Quantitative Results

We evaluated our method on the same datasets used by 3DGS, namely: Mip-NeRF360 [3], TanksAndTemples [20], and DeepBlending [15]. For each test, we report image

quality metrics (PSNR, SSIM, LPIPS, computed on VGG), the model size in megabytes (SIZE), the number of primitives $|\mathcal{G}_{L-1}|$ (here W for brevity), and the average frame rate on the test set (FPS). We present the results for each architecture, comparing them with various state-of-the-art proposals. To ensure a fair comparison, all the methods were re-trained and evaluated on our machine, for known discrepancies in reported results as noted by [4]. Additionally, some methods were re-trained using updated hyperparameters to generate rate-distortion curves in alignment with the parameters specified in their respective papers. The main results are summarized in Tab. 1. In Fig. 3, we plot rate-distortion and PSNR/FPS curves. These findings show that our method is generally competitive with current state-of-the-art approaches while benefiting from being a scalable model, as our rate/distortion curve is generated instantly. We divide our analysis of the results between neural-based 3DGS models and explicit ones, as the former generally provides superior rate-distortion performance.

Neural-based 3DGS To the best of our knowledge, HAC [6] represents the current state-of-the-art in terms of rate distortion. HAC uses the Scaffold-GS [24] codebase. Scaffold-GS provides slightly higher reconstruction quality than 3DGS (approximately +0.3 dB) while reducing storage by about 5 \times . By applying our method to Scaffold-GS we observe that it delivers comparable results, slightly outperforming HAC on the MipNeRF-360 dataset, while HAC remains superior on the Tanks&Temples dataset. We consider our results competitive, as our scalable compression method does not require re-training, unlike other methods that need to train a separate model with different hyperparameters. Our method offers another advantage beyond scalability: by masking a higher number of anchor points on average, our model is faster, achieving a frame rate increase ranging from +33% to +62% while maintaining similar reconstruction quality.

Explicit 3DGS Regarding the comparison with explicit Gaussian splatting models, our results are state-of-the-art on nearly every dataset in terms of rate/distortion and performance at equivalent or even superior quality, achieving up to a 3 \times increase in FPS. There is one point where CompGS [22] slightly outperforms our method, but this approach scales less effectively at higher compression rates. In this case, our approach also offers the advantage of utilizing a single scalable model, which eliminates the need for re-training when adapting to different compression rates. Notably, the models obtained with our method are highly scalable, ranging from an extremely high compression rate of a few megabytes to an extremely low one.

Table 1. Comparison of our methods against recent methods. All methods have been retrained and tested on the same hardware. For clarity, we present four compression levels out of 8 for our configurations, selected to match the compression rate of the other methods. These levels, labeled as *Ours*, are derived from the same model without the need for retraining (in contrast to the other approaches). Red, orange and yellow respectively indicates the first, second and third best result.

Method	Mip-NeRF360						Tanks&Temples						Deep Blending					
	PSNR↑	SSIM↑	LPiPS↓	Size[MB]↓	W↓	FPS↑	PSNR↑	SSIM↑	LPiPS↓	Size[MB]↓	W↓	FPS↑	PSNR↑	SSIM↑	LPiPS↓	Size[MB]↓	W↓	FPS↑
HAC (low) [6]	27.78	0.812	0.277	22.0	502	68	24.37	0.853	0.215	11.1	307	88	30.34	0.909	0.329	6.3	190	166
HAC (high) [6]	27.53	0.807	0.290	15.2	426	72	24.05	0.846	0.222	7.9	300	85	29.98	0.904	0.340	4.1	188	173
RDO [34]	27.05	0.801	0.288	23.3	1860	178	23.32	0.839	0.232	11.9	912	257	29.72	0.906	0.318	18.0	1478	200
LightGaussian [10]	27.24	0.810	0.273	51.0	2197	161	23.55	0.839	0.235	28.5	1210	225	29.41	0.904	0.329	43.2	956	348
SOG [26]	27.08	0.799	0.277	40.3	2176	132	23.56	0.837	0.221	22.8	1242	227	29.26	0.894	0.336	17.7	890	236
Compact-3DGS [21]	27.02	0.800	0.287	29.1	1429	108	23.41	0.836	0.238	20.9	842	147	29.76	0.905	0.324	23.8	1053	144
Reduced-3DGS [31]	27.19	0.810	0.267	29.3	1436	234	23.55	0.843	0.223	14.0	656	358	29.70	0.907	0.315	18.3	990	304
EAGLES [14]	27.13	0.809	0.278	57.1	1290	156	23.20	0.837	0.241	28.9	651	227	29.75	0.910	0.318	52.4	1192	144
Comp-GS [22]	27.28	0.802	0.283	16.4	485	165	23.62	0.837	0.248	9.8	241	286	29.89	0.904	0.336	10.0	246	253
Ours w/ Scaffold-GS	27.75	0.810	0.284	19.7	453	98	24.01	0.846	0.226	11.0	266	142	30.34	0.909	0.331	8.4	63	212
	27.59	0.803	0.297	14.1	369	107	23.95	0.843	0.234	8.9	230	156	30.29	0.908	0.334	7.2	56	208
	27.34	0.793	0.316	10.3	288	127	23.85	0.837	0.244	7.3	196	176	30.14	0.905	0.343	5.3	44	225
	27.07	0.780	0.336	7.5	221	146	23.72	0.830	0.258	5.9	165	189	29.76	0.897	0.358	3.9	33	236
Ours w/ 3DGS-MCMC	27.42	0.815	0.263	43.9	1546	146	23.97	0.842	0.220	22.2	938	216	29.71	0.901	0.323	19.5	931	263
	27.23	0.804	0.289	20.0	603	222	23.76	0.831	0.241	11.8	438	311	29.70	0.901	0.326	11.0	491	345
	26.99	0.790	0.312	13.4	381	268	23.49	0.821	0.259	8.6	301	366	29.66	0.901	0.331	8.3	357	391
	26.59	0.772	0.339	9.0	242	317	23.06	0.806	0.281	6.3	208	426	29.56	0.897	0.348	4.8	189	488
Ours w/ 3DGS	27.27	0.807	0.273	40.5	1546	189.1	23.76	0.839	0.231	21.1	938	269	29.73	0.904	0.327	19.8	931	302
	27.16	0.801	0.295	18.3	603	270	23.66	0.832	0.245	11.6	438	383	29.73	0.903	0.334	10.1	491	425
	26.93	0.791	0.315	12.0	381	317	23.48	0.824	0.259	8.6	301	439	29.74	0.902	0.340	7.2	357	492
	26.55	0.773	0.341	7.9	242	371	23.13	0.812	0.279	6.4	208	509	29.67	0.899	0.348	5.1	189	564

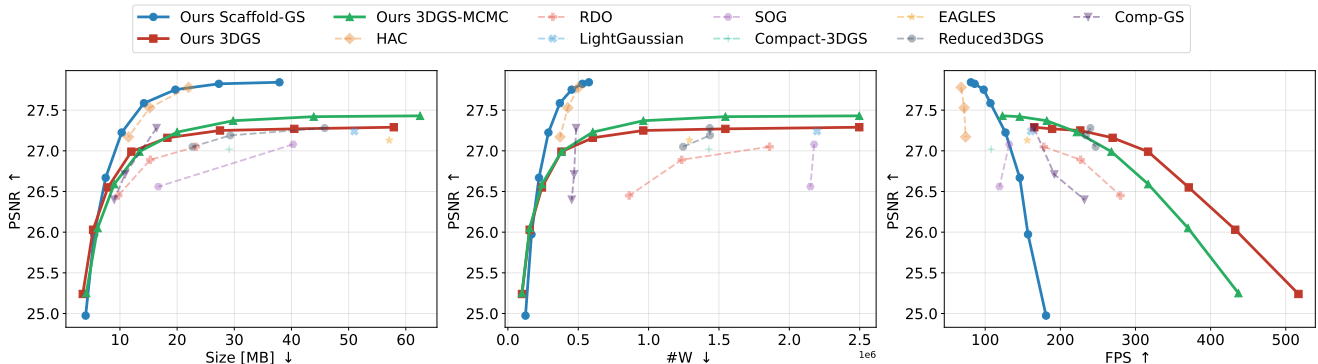


Figure 3. Rate-distortion curves (left), PSNR/W (center, where W is the number of primitives) and PSNR/FPS (right) curve on Mip-NeRF360. Our approach achieves competitive results with both neural-based Gaussian models and explicit ones while maintaining significantly higher speed at comparable quality. It is also the only method that achieves scalability without requiring ad-hoc training.

4.3. Visualizing LoDs

In Fig. 4 we visualize some LoD levels for various scenes. For each LoD level, we report the average frame rate computed for rendering the image of the test set, the number of Gaussians, the average PSNR, and the model size. The transition between LoDs is smooth thanks to the fine-tuning process with random LoD sampling. Moreover, we observe that lower LODs are extremely fast and small, with rendering speeds exceeding 800 FPS and model sizes as low as 2.4MB for the *drjohnson* scene from the DeepBlending dataset (in comparison with the vanilla-3DGS which renders the same scene at 146FPS and requires 780MB of storage). Similar performances are achieved across other datasets. It is important to note that lower LoDs tend to lose fine details, particularly in high-frequency areas such as reflections, transparency handling, and background elements.

This is particularly noticeable in the *kitchen* scene, where at lower levels of detail the glass bottle in the background is either not rendered at all or only partially and becomes progressively more defined at higher levels. Another example can be seen in the *counter* scene, with the reflection on the dishes. Other examples are the paining in the *drjohnson* scene and the trees in the background of the *truck* scene. This is a significant result, demonstrating the effectiveness of the method, which automatically learns a hierarchy and preserves the most important details at each level, minimizing the loss of detail to secondary aspects. This is further illustrated in Fig. 5, where we render only the Gaussian associated with an enhancement level. As the level increases, we observe that the Gaussians focus on more complex geometry and finer details.



Figure 4. Visualization of LoDs. For visual purposes, we show the first three LoD levels and the last one. For each LoD we provide the average FPS, PSNR, primitives count W (in thousands), and size. Starting from top to bottom we have: *kitchen*, *counter*, *drjohnson* and *truck* scenes.



Figure 5. Visualization of enhancement levels. We render only the Gaussians belonging to the specified enhancement level.

4.4. Ablations

Here, we investigate how different choices of parameters and algorithms affect the render quality. These choices include the number of levels L , the ranking methods used to build the masks, the impact of compression, and the hierarchy on quality.

4.4.1. Number of levels

In our configuration, we opted for $L = 8$ levels. However, we tested our method with a variable number of levels and observed minimal differences in performance. Fig. 6 shows that, with increasing number of levels, there is a slight de-

crease in the quality of lower LoDs, while the quality in higher levels remains similar. We chose 8 levels as a good balance, but our method is easily extendable to a higher number of levels without significant loss in quality. This highlights the scalability of our approach.

4.4.2. Pruning methods

In Fig. 7, we investigate multiple strategies for ranking Gaussians, which are commonly used to prune and compact the model. We found that our method provides better reconstruction quality with the same number of Gaussians compared to several proposed strategies, such as those based on opacity [17] or positional gradient [1]. Additionally, we compared our technique with the one proposed by Light-Gaussian [10] and still achieved superior results. All these methods have been tested using the same iterative process. We also evaluated the necessity of iterative masking versus the same ranking method but applied in a one-shot manner labeled as *Ours (One Shot)*, where the gradient is accumulated only once to create the levels. Our experiments demonstrate the importance of the iterative approach, as the one-shot method leads to a loss in quality, particularly at lower LoDs. Since the iterative masking process is very

fast, we opted to use the sum of the gradient norms of the parameters as a score and perform the masking iteratively.

Table 2. Effects of fine-tuning and compression on Mip-NeRF360.

LoD	W	Mask Only			Fine Tuning			Fine-Tuning + Compression		
		PSNR \uparrow	SSIM \uparrow	Size[MB] \downarrow	PSNR \uparrow	SSIM \uparrow	Size[MB] \downarrow	PSNR \uparrow	SSIM \uparrow	Size[MB] \downarrow
0	100	18.52	0.553	24.1	25.20	0.719	24.1	25.24	0.717	3.5
1	155	19.90	0.606	36.7	26.06	0.752	36.7	26.03	0.749	5.3
2	242	21.52	0.662	56.4	26.65	0.778	56.4	26.55	0.773	7.9
3	381	23.28	0.715	89.1	26.84	0.787	89.1	26.93	0.791	12.0
4	603	25.00	0.760	142.8	27.08	0.796	142.8	27.16	0.801	18.3
5	962	26.45	0.793	216.6	27.33	0.807	69.8	27.25	0.806	27.5
6	1546	27.23	0.810	365.9	27.45	0.813	227.2	27.27	0.807	40.5
7	2497	27.49	0.815	562.2	27.47	0.814	365.6	27.29	0.808	57.9
AVG	811	23.67	0.714	186.7	26.76	0.783	126.5	26.72	0.781	21.6

4.4.3. Effects of Fine-Tuning and Compression

We analyze the effects of fine-tuning and compression from both a quantitative and qualitative perspective. As shown in Tab. 2, the fine-tuning phase significantly improves reconstruction quality, particularly for lower LoDs, while slightly reducing quality in the two highest LoDs, of about 0.02 dB. Regarding compression, we observe a reduction in storage ranging from 99.37% to 89.69%, depending on the level considered. The impact on reconstruction quality is minimal, with a loss of 0.03 dB to 0.18 dB across different levels. In Fig. 9, we also visualize the visual impact of fine-tuning. Non-fine-tuned models exhibit holes and generally lower quality, while the LoDs after fine-tuning show improved quality with way fewer artifacts.

4.4.4. Impact of hierarchical representation

In this ablation study, we evaluate our hierarchical compression method against a non-hierarchical variant to assess how much our hierarchical approach diverges from the best achievable performance. Specifically, we re-run our method but omit any hierarchy constraints. The process is as follows: we accumulate gradients for one epoch, mask the k Gaussians with the lowest gradient values, perform a fine-tuning cycle of 7,000 iterations, and evaluate the performance (each evaluation is a point in Fig. 8). This procedure is repeated across 8 levels, down to a minimum threshold of 100,000 parameters, with each level acting as an independent model. Interestingly, our method sets a new performance benchmark, outperforming HAC and underline the effectiveness of iterative, gradient-based pruning for this task. Our hierarchical version, though also superior to HAC, performs less well, particularly at high compression levels. This is due to the imposed hierarchy, which requires optimizing each level in relation to the others, thus introducing a trade-off between higher and lower levels.

5. Limitation and Future Work

Our approach demonstrates effectiveness in scalable compression tasks, matching or even surpassing the performance of non-scalable compression methods. However, it

also inherits certain limitations typical of top-down pruning and compression approaches, such as the requirement for a pre-trained model with a well-established geometric prior. In future work, we intend to explore the potential for a bottom-up approach, integrating the hierarchical structure during the training of the Gaussian model.

6. Conclusion

This paper presented GoDe, a framework for a progressive level of detail and scalable compression. Our extensive experiments show that our method is highly scalable and competitive, often surpassing non-scalable state-of-the-art techniques in both quality and performance. In fact, unlike previously proposed methods, our approach allows for model compression at multiple rates without the need for retraining with different hyperparameters. This framework also enables adaptive rendering: given the hierarchical-layered structure of the model, it is possible to dynamically select Gaussians up to a certain level to meet specific criteria, such as a target frame rate. Additionally, a notable advantage of our approach is its generality: relying on widely applicable techniques, such as gradient-informed pruning, our method can be integrated into popular 3DGS models.

References

- [1] Muhammad Salman Ali, Maryam Qamar, Sung-Ho Bae, and Enzo Tartaglione. Trimming the fat: Efficient compression of 3d gaussian splats through pruning. *arXiv preprint arXiv:2406.18214*, 2024. 2, 3, 7
- [2] Milena T. Bagdasarian, Paul Knoll, Yi-Hsin Li, Florian Barthel, Anna Hilsman, Peter Eisert, and Wieland Morgenstern. 3dgs.zip: A survey on 3d gaussian splatting compression methods, 2024. 2
- [3] Jonathan T Barron, Ben Mildenhall, Dor Verbin, Pratul P Srinivasan, and Peter Hedman. Mip-nerf 360: Unbounded anti-aliased neural radiance fields. In *Proceedings of the IEEE/CVF Conference on Computer Vision and Pattern Recognition*, pages 5470–5479, 2022. 5
- [4] Samuel Rota Bulò, Lorenzo Porzi, and Peter Kontschieder. Revising densification in gaussian splatting. *arXiv preprint arXiv:2404.06109*, 2024. 5
- [5] Anpei Chen, Zexiang Xu, Andreas Geiger, Jingyi Yu, and Hao Su. Tensorf: Tensorial radiance fields. *ECCV*, 2022. 1, 3
- [6] Yihang Chen, Qianyi Wu, Weiyao Lin, Mehrtash Harandi, and Jianfei Cai. Hac: Hash-grid assisted context for 3d gaussian splatting compression. In *European Conference on Computer Vision*, 2024. 3, 5, 6
- [7] T.M. Cover and J.A. Thomas. *Elements of Information Theory*. Wiley, 2012. 4
- [8] Chenxi Lola Deng and Enzo Tartaglione. Compressing explicit voxel grid representations: fast nerfs become also small. In *Proceedings of the IEEE/CVF Winter Conference on Applications of Computer Vision*, pages 1236–1245, 2023. 3

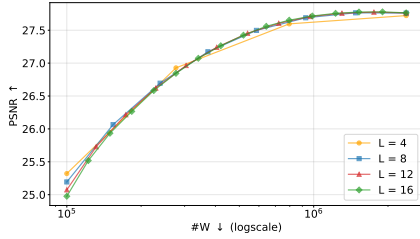


Figure 6. Ablation on the number of levels on Mip-NeRF360.

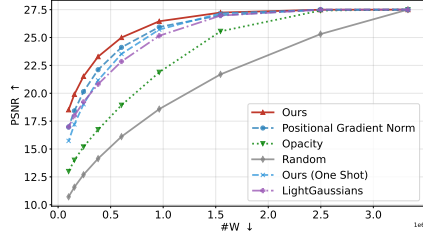


Figure 7. Comparison among pruning methods on Mip-NeRF 360.

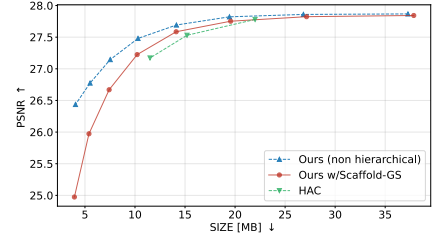


Figure 8. Comparison among our method with Scaffold-GS, a non-scalable variant of the same method and HAC. This constitutes an upper bound to our scalable method.



Figure 9. Effects of fine-tuning on the train scene of *Tanks&Temples* dataset. In the first row, LoDs without fine-tuning; on the second, LoDs after fine-tuning.

[9] Francesco Di Sario, Riccardo Renzulli, Enzo Tartaglione, and Marco Grangetto. Boost your nerf: A model-agnostic mixture of experts framework for high quality and efficient rendering. In Aleš Leonardis, Elisa Ricci, Stefan Roth, Olga Russakovsky, Torsten Sattler, and Gül Varol, editors, *Computer Vision – ECCV 2024*, pages 176–192, Cham, 2025. Springer Nature Switzerland. 3

[10] Zhiwen Fan, Kevin Wang, Kairun Wen, Zehao Zhu, De-jia Xu, and Zhangyang Wang. Lightgaussian: Unbounded 3d gaussian compression with 15x reduction and 200+ fps. *arXiv preprint arXiv:2311.17245*, 2023. 3, 6, 7

[11] Guangchi Fang and Bing Wang. Mini-splatting: Representing scenes with a constrained number of gaussians. In Aleš Leonardis, Elisa Ricci, Stefan Roth, Olga Russakovsky, Torsten Sattler, and Gül Varol, editors, *Computer Vision – ECCV 2024*, pages 165–181, Cham, 2024. Springer Nature Switzerland. 2

[12] Sara Fridovich-Keil, Giacomo Meanti, Frederik Rahbæk Warburg, Benjamin Recht, and Angjoo Kanazawa. K-planes: Explicit radiance fields in space, time, and appearance. In *2023 IEEE/CVF Conference on Computer Vision and Pattern Recognition (CVPR)*, pages 12479–12488, 2023. 1

[13] Sara Fridovich-Keil, Alex Yu, Matthew Tancik, Qinlong Chen, Benjamin Recht, and Angjoo Kanazawa. Plenoxels: Radiance fields without neural networks. In *Proceedings of the IEEE/CVF Conference on Computer Vision and Pattern Recognition*, pages 5501–5510, 2022. 1, 3

[14] Sharath Girish, Kamal Gupta, and Abhinav Shrivastava. Eagles: Efficient accelerated 3d gaussians with lightweight encodings, 2024. 2, 3, 6

[15] Peter Hedman, Julien Philip, True Price, Jan-Michael Frahm,

George Drettakis, and Gabriel Brostow. Deep blending for free-viewpoint image-based rendering. *37(6):257:1–257:15*, 2018. 5

[16] Wenbo Hu, Yuling Wang, Lin Ma, Bangbang Yang, Lin Gao, Xiao Liu, and Yuewen Ma. Tri-miprf: Tri-mip representation for efficient anti-aliasing neural radiance fields. In *Proceedings of the IEEE/CVF International Conference on Computer Vision*, pages 19774–19783, 2023. 1

[17] Bernhard Kerbl, Georgios Kopanas, Thomas Leimkühler, and George Drettakis. 3d gaussian splatting for real-time radiance field rendering. *ACM Transactions on Graphics*, 42(4), 2023. 1, 2, 5, 7

[18] Bernhard Kerbl, Andreas Meuleman, Georgios Kopanas, Michael Wimmer, Alexandre Lanvin, and George Drettakis. A hierarchical 3d gaussian representation for real-time rendering of very large datasets. *ACM Transactions on Graphics*, 43(4), July 2024. 3

[19] Shakiba Kheradmand, Daniel Rebain, Gopal Sharma, Weiwei Sun, Jeff Tseng, Hossam Isack, Abhishek Kar, Andrea Tagliasacchi, and Kwang Moo Yi. 3d gaussian splatting as markov chain monte carlo. *arXiv preprint arXiv:2404.09591*, 2024. 5

[20] Arno Knapitsch, Jaesik Park, Qian-Yi Zhou, and Vladlen Koltun. Tanks and temples: Benchmarking large-scale scene reconstruction. *ACM Transactions on Graphics (ToG)*, 36(4):1–13, 2017. 5

[21] Joo Chan Lee, Daniel Rho, Xiangyu Sun, Jong Hwan Ko, and Eunbyung Park. Compact 3d gaussian representation for radiance field. *arXiv preprint arXiv:2311.13681*, 2023. 3, 6

[22] Xiangrui Liu, Xinju Wu, Pingping Zhang, Shiqi Wang, Zhu Li, and Sam Kwong. Compgs: Efficient 3d scene representation via compressed gaussian splatting. In *Proceedings of the 32nd ACM International Conference on Multimedia*, pages 2936–2944, 2024. 3, 5, 6

[23] Yang Liu, Chuanchen Luo, Lue Fan, Naiyan Wang, Junran Peng, and Zhaoxiang Zhang. Citygaussian: Real-time high-quality large-scale scene rendering with gaussians. In Aleš Leonardis, Elisa Ricci, Stefan Roth, Olga Russakovsky, Torsten Sattler, and Gül Varol, editors, *Computer Vision – ECCV 2024*, pages 265–282, Cham, 2025. Springer Nature Switzerland. 2

[24] Tao Lu, Mulin Yu, Linning Xu, Yuanbo Xiangli, Limin Wang, Dahua Lin, and Bo Dai. Scaffold-gs: Structured 3d gaussians for view-adaptive rendering. In *Proceedings of*

- the *IEEE/CVF Conference on Computer Vision and Pattern Recognition (CVPR)*, pages 20654–20664, June 2024. 3, 5
- [25] Ben Mildenhall, Pratul P Srinivasan, Matthew Tancik, Jonathan T Barron, Ravi Ramamoorthi, and Ren Ng. Nerf: Representing scenes as neural radiance fields for view synthesis. In *European conference on computer vision*, pages 405–421. Springer, 2020. 1
- [26] Wieland Morgenstern, Florian Barthel, Anna Hilsmann, and Peter Eisert. Compact 3d scene representation via self-organizing gaussian grids. *arXiv preprint arXiv:2312.13299*, 2023. 6
- [27] Thomas Müller, Alex Evans, Christoph Schied, and Alexander Keller. Instant neural graphics primitives with a multiresolution hash encoding. *ACM Trans. Graph.*, 41(4):102:1–102:15, July 2022. 1
- [28] Thomas Müller, Alex Evans, Christoph Schied, and Alexander Keller. Instant neural graphics primitives with a multiresolution hash encoding. *ACM Transactions on Graphics (ToG)*, 41(4):1–15, 2022. 3
- [29] KL Navaneet, Kossar Pourahmadi Meibodi, Soroush Abbasi Koohpayegani, and Hamed Pirsiavash. Compgs: Smaller and faster gaussian splatting with vector quantization. *ECCV*, 2024. 2
- [30] Simon Niedermayr, Josef Stumpfegger, and Rüdiger Westermann. Compressed 3d gaussian splatting for accelerated novel view synthesis. In *Proceedings of the IEEE/CVF Conference on Computer Vision and Pattern Recognition*, pages 10349–10358, 2024. 3, 5
- [31] Panagiotis Papantonakis, Georgios Kopanas, Bernhard Kerbl, Alexandre Lanvin, and George Drettakis. Reducing the memory footprint of 3d gaussian splatting. *Proceedings of the ACM on Computer Graphics and Interactive Techniques*, 7(1):1–17, 2024. 3, 4, 6
- [32] Michael Seufert, Sebastian Egger, Martin Slanina, Thomas Zinner, Tobias Hoßfeld, and Phuoc Tran-Gia. A survey on quality of experience of http adaptive streaming. *IEEE Communications Surveys & Tutorials*, 17(1):469–492, 2014. 5
- [33] Cheng Sun, Min Sun, and Hwann-Tzong Chen. Direct voxel grid optimization: Super-fast convergence for radiance fields reconstruction. In *Proceedings of the IEEE/CVF Conference on Computer Vision and Pattern Recognition*, pages 5459–5469, 2022. 1, 3
- [34] Henan Wang, Hanxin Zhu, Tianyu He, Runsen Feng, Jiajun Deng, Jiang Bian, and Zhibo Chen. End-to-end rate-distortion optimized 3d gaussian representation. *arXiv preprint arXiv:2406.01597*, 2024. 3, 6
- [35] Minye Wu and Tinne Tuytelaars. Implicit gaussian splatting with efficient multi-level tri-plane representation, 2024. 3
- [36] Shuzhao Xie, Weixiang Zhang, Chen Tang, Yunpeng Bai, Rongwei Lu, Shijia Ge, and Zhi Wang. Mesongs: Post-training compression of 3d gaussians via efficient attribute transformation. In *European Conference on Computer Vision*. Springer, 2024. 3
- [37] Shuzhao Xie, Weixiang Zhang, Chen Tang, Yunpeng Bai, Rongwei Lu, Shijia Ge, and Zhi Wang. Mesongs: Post-training compression of 3d gaussians via efficient attribute transformation. In Aleš Leonardis, Elisa Ricci, Stefan Roth, Olga Russakovsky, Torsten Sattler, and Gül Varol, editors, *Computer Vision – ECCV 2024*, pages 434–452, Cham, 2025. Springer Nature Switzerland. 2
- [38] Zhiwen Yan, Weng Fei Low, Yu Chen, and Gim Hee Lee. Multi-scale 3d gaussian splatting for anti-aliased rendering. In *Proceedings of the IEEE/CVF Conference on Computer Vision and Pattern Recognition (CVPR)*, pages 20923–20931, June 2024. 2
- [39] M. Zwicker, H. Pfister, J. van Baar, and M. Gross. Ewa volume splatting. In *Proceedings Visualization, 2001. VIS '01.*, pages 29–538, 2001. 2